Electron Capture by $C_{60}F_{35}{}^-$ in Collisions with Atomic and Molecular Targets

O. V. Boltalina,[1] P. Hvelplund,[2] M. C. Larsen,[2] and M. O. Larsson[2]
[1]*Chemistry Department, Moscow State University, Moscow 119899, Russia*
[2]*Institute of Physics and Astronomy, University of Aarhus, DK-8000 Aarhus C, Denmark*
(Received 17 September 1997)

We have studied nondissociative and dissociative electron capture by $C_{60}F_{35}{}^-$ in collisions with various gas targets. It is argued that this endoergic capture process can be interpreted within a curve-crossing model of the Landau-Zener type. Cross sections as large as 10^{-16} cm^2 are measured for electron capture by 50 keV $C_{60}F_{35}{}^-$ in collisions with Xe. [S0031-9007(98)06313-3]

PACS numbers: 36.40.–c, 34.70.+e, 61.46.+w, 82.30.Fi

Charge transfer or electron capture in collisions between energetic ions and atoms constitute an important branch of reactions in atomic physics. During the collision, the electron clouds around the interacting particles are brought into "oscillations" and as a result one or more electrons may change their affiliations. The probability that an electron ends up in an eigenstate on the counterpart in the collision has to be estimated taking into consideration the exchange of translational energy to internal energy, or coupling to the radiation field. Charge transfer or electron capture in atomic collisions plays a decisive role in astrophysics, controlled thermonuclear fusion research, and in accelerator-trap or storage-ring based physics [1,2].

Recently, the group of interacting particles has been broadened considerably, and charge transfer in cluster-cluster collisions [3,4] and in interactions involving large polypeptides and proteins [5] have been reported. Fluorinated fullerenes are now routinely produced, and some have been isolated and characterized [6,7]. $C_{60}F_{48}$ can be brought into the gas phase by thermal desorption. Anions with a conserved molecular structure, $C_{60}F_{48}{}^-$, may then be formed either as a result of surface thermal ionization [8] or by capture of thermal electrons. Under more violent conditions, e.g., laser desorption [9] or the technique used in the present work (see below), the anion formation from $C_{60}F_{48}$ is dissociative, and odd-numbered $C_{60}F_n{}^-$ ions are found to be the most abundant. Sequential attachment of two low-energy electrons resulting in doubly charged $C_{60}F_{48}$ anions has been observed, and the first and second electron affinities were calculated to be 5.07 and 2.27 eV, respectively [10]. Here we address electron capture in collisions between 50 keV $C_{60}F_{35}{}^-$ and atomic and molecular gases. This particular projectile ion was chosen because it was the heaviest relative abundant fluorinated fullerene anion produced in our ion source. Since the active electron is bound with 10 eV or more in the target atom or molecule and only with ~2 eV in the product dianion, the charge transfer process is strongly endoergic, and translational energy has to be converted into internal energy. In the case of dissociative electron capture, even more translational energy (~4 eV per lost fluorine atom) [8,11] has to be converted. It should be noted that in conventional low-energy collisions, capture takes place only when the process is exoergic [12]. This observation can most easily be "envisaged" by considering the capture process as a transition between potential energy curves pertaining to initial and final states [13]. When a multiply charged ion captures an electron from a neutral atom, both ions are positive in the exit state, but in the present case the ions have opposite charge and, hence, a curve-crossing model applies for an endoergic charge transfer process. Similar arguments have been used in order to explain double capture by singly charged cations in collisions with neutral atoms [14].

The $C_{60}F_{48}$ sample was prepared in a reaction of C_{60} (99.9%) with elemental fluorine at 315 °C, as described in Ref. [7]. The purity and molecular composition were controlled by the elemental chemical analysis ($C_{60}F_{48\pm1}$), mass spectrometry, and high-pressure liquid chromatography. The ^{19}F NMR spectrum on this sample was identical to the one published previously [6,7] indicating that the compound represents a single structural isomer (two chiral forms of D_3 symmetry).

The experimental arrangement used for these investigations has been described elsewhere [3]. In the present experiment, $C_{60}F_{48}$ powder was heated to ~200 °C in an oven attached to our conventional ion source [15]. The filament temperature was only 1500 °C, and the dominating anion formation process is believed to be a dissociative surface attachment on the hot tungsten filament. The anions were extracted from the ion source and electrostatically accelerated to an energy of 50 keV. The energetic cluster ions were magnetically mass selected before entering the 3 cm long target cell. After exiting the target, the nonreacted primary ions and all fragment anions were electrostatically deflected into a single particle counter (channeltron) by a 180° hemispherical analyzer. Mass spectra were obtained by sweeping the analyzer voltage, since all ions have approximately the same velocity at these high collision energies. Figure 1 shows a so-called magnet scan obtained for zero target pressure and for a fixed analyzer voltage (primary ions), but for a varying magnetic field. The peak heights in this spectrum reflect the relative intensities of cluster ions

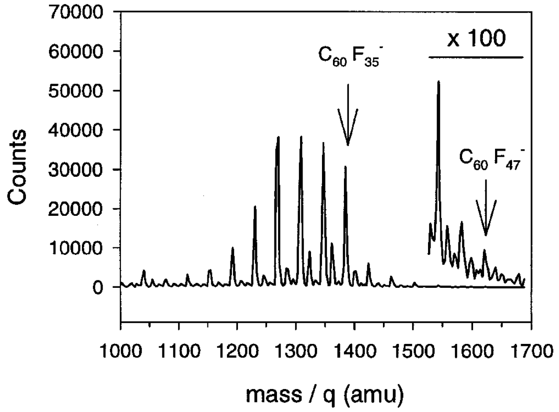

FIG. 1. Magnet scan showing relative intensity of ions extracted from the ion source.

produced in the ion source. The most intense beams are the odd-numbered fluorine ions with between 25 and 35 fluorine atoms attached to the C_{60} cage, whereas the ions with higher fluorine content up to $C_{60}F_{47}^-$ have much lower intensities. For comparison, in the electron impact mass spectrum of the same sample obtained under equilibrium conditions (Knudsen Cell Mass Spectrometry), $C_{60}F_{48}^+$ comprised about 90% of the total intensity [16]. This indicates that more vehement ionization conditions were used in the present work. It is also remarkable that a sharp cutoff in the intensity is seen after the $C_{60}F_{36}^-$ peak. This confirms earlier theoretical predictions [17,18] and experimental observations [19,20] on the particular stability of the fullerene with 36 addends for both hydrogenated and fluorinated derivatives. For the latter, it is not only the high symmetrical structure that indicates its enhanced stability but also the strength of the C-F bond. $C_{60}F_{35}^-$ was chosen for our further experiments on the collisions with various gas targets. Figure 2 shows a "fragmentation" spectrum (negative ions) obtained when the $C_{60}F_{35}^-$ is passed through a Xe target. The dominating peaks, apart from the peak corresponding to the primary beam, correspond to the loss of an even number of fluorine atoms, but two peaks at around half of the deflection voltage, necessary to deflect the primary beam, are assigned to $C_{60}F_{34}^{--}$ and $C_{60}F_{35}^{--}$ resulting from electron capture in the Xe target gas. From similar spectra at various target pressures for the gases NO, O_2, Xe, CH_4, H_2, Ar, and He, cross sections for nondissociative capture,

$$C_{60}F_{35}^- + X \rightarrow C_{60}F_{35}^{--} + X^+ - \Delta E\,, \qquad (1)$$

and dissociative capture,

$$C_{60}F_{35}^- + X \rightarrow C_{60}F_{34}^{--} + X^+ + \mathrm{F} - \Delta E\,, \qquad (2)$$

were obtained. ΔE is the energy defect in the reaction. The cross sections obtained are listed in Table I, and both the relative and absolute sizes are found to depend strongly on the nature of the target gas.

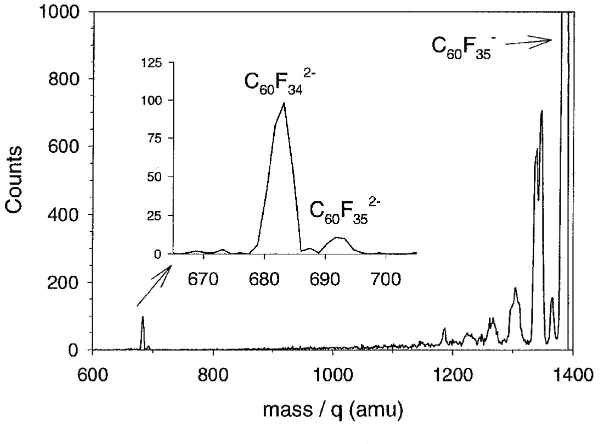

FIG. 2. Mass divided by charge (m/q) spectrum for negative "fragments" resulting from collisions between $C_{60}F_{35}^-$ and Xe. The heavy fragment peaks reflect loss of F_1, F_2, FC_2, F_4, etc. The inset displays the dianion region.

We consider the capture reaction (1) in terms of two quasimolecules $[C_{60}F_{35}^- X]$ and $[C_{60}F_{35}^{--} X^+]$. The long range potential energy function of the former quasimolecule may be assumed to be independent of the intermolecular separation r (distance between X and the center of $C_{60}F_{35}$). In the exit channel, the potential energy function contains three terms: first the Coulomb attraction between the two ions, then an attraction due to the large polarizability α [10] of the $C_{60}F_{35}^{--}$ ions, and third, the endoergicity term ΔE. The form as a function of the intermolecular separation r is given approximately by

$$V(r) = -\frac{2}{r} - \frac{a^3}{2r^2(r^2 - a^2)} + \Delta E\,, \qquad (3)$$

where $a \sim 5$ Å is the radius of the assumed conducting spherical $F_{35}C_{60}^{--}$ molecule. The two potential energy functions for $\Delta E = 10$ eV are shown in Fig. 3. It should be noted that the curve crossings take place just outside the cluster surface when the cluster is approximated by a conducting sphere.

The electron capture process can be considered in terms of two adiabatic curves (dotted lines), which undergo a pseudocrossing at an internuclear separation around R_c. The standard Landau-Zener approximation can, in principle, be used to determine the reaction transition probabilities [13] and, hence, the cross section for the process. We are aware that the curve-crossing description of capture in this context, especially in the case of dissociative electron capture, is rather defective, but despite this the model indicates the type of interaction which results in formation of doubly charged negative ions.

Unlike the case in electron capture by multiply charged positive atomic ions, the dominating reaction channels in the present case are leading to fragmentation of the large molecular ion. This statement is supported by the spectrum shown in Fig. 2, where fragmentation is seen to be the dominating process. It should also be added that

TABLE I. Capture cross sections (nondissociative and dissociative) for collisions between $C_{60}F_{35}^-$ and the listed target gases along with the target gas ionization potentials I_I.

Target gas	Ionization potential I_I (eV)	Nondissociative capture cross section (cm^2)	Dissociative capture cross section (cm^2)
H_2	15.4	7.1×10^{-18}	2.4×10^{-17}
He	24.6	$<10^{-18}$	$<10^{-18}$
CH_4	13.0	2.2×10^{-17}	1.4×10^{-16}
NO	9.3	4.1×10^{-17}	7.1×10^{-17}
O_2	12.1	1.2×10^{-17}	8.3×10^{-17}
Ar	15.8	8.1×10^{-18}	1.8×10^{-17}
Xe	12.1	3.1×10^{-17}	1.2×10^{-16}

neutral and positive fragments are much more abundant than negative ones, implying that fragmentation is really the dominating process in the collisions discussed here. Hence, electron capture occurs only for a very narrow range of impact parameters, ranging from near the cage radius and out the curve crossing distance (~6 Å). This explains why the measured cross sections amount to only 1% of the geometrical cross section.

The simplest way of displaying the measured capture cross section values listed in Table I is to plot them as a function of the target ionization potential or alternatively as a function of the electronic endoergicity of the process. In Fig. 4, the cross section for the processes (1) and (2) are both plotted as a function of the endoergicity which is found as the difference in potential energy of the active electron before and after the transfer takes place; i.e., $\Delta E \approx I_I - 2$ eV, where I_I is the target ionization potential. The cross section for nondissociative capture decreases monotonically with increasing endoergicity, whereas the cross section for dissociative capture attains a maximum value for ΔE around 10 eV. How to exactly model the differences between dissociative and nondissociative electron capture processes is not clear at present. We have therefore chosen to plot the capture cross section as a function of the electronic endoergicity, also for the dissociative capture process, and not to add the dissociation energy. Furthermore, the problem about the relative importance of one- and two-step processes in dissociative electron capture has to await further investigation.

Aspects of the cross section behavior illustrated in Fig. 4 could be introduced as follows: For initially very strongly bound electrons (He), the impact parameter distance where electron capture could take place would lead to severe destruction of the fullerene cage and, hence, a small probability for electron capture. On the other hand, very loosely bound target electrons, which can be considered quasifree, would have too little kinetic energy to pass the Coulomb barrier around the projectile anion—again resulting in small electron capture cross sections. Electron capture will therefore most likely take place for moderately bound electrons.

We assume that the temperature of the projectile $C_{60}F_{35}^-$ is low compared to that of C_{60}^- (~2000 K) extracted from the same ion source [21]. This assumption is built on experimental findings by Steger *et al.* [22] albeit for neutral fluorinated fullerenes. Steger *et al.* showed that hot fluorinated fullerenes have a larger proclivity for fragmentation than normal fullerenes. We therefore argue that the projectile ions exiting the ion source, due to evaporative cooling, possess only a small amount of

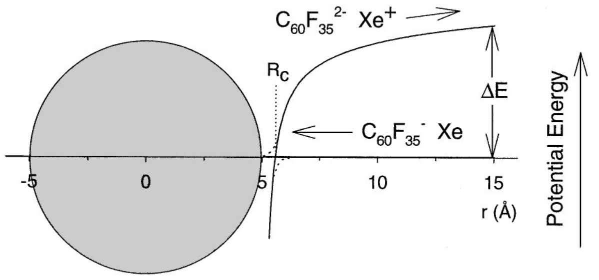

FIG. 3. Potential energy curves for the quasimolecules $C_{60}F_{35}^-$ Xe and $C_{60}F_{35}^{--}$ Xe$^+$ as a function of the distance between the two ions. ΔE is the endoergicity of the electron capture reaction which occurs at a distance R_c between the two centers. The dashed curves represent a pseudocrossing of adiabatic potential energy curves pertaining to low-velocity collisions, and the shaded area relates to the size of the $C_{60}F_{35}$ fluorofullerene.

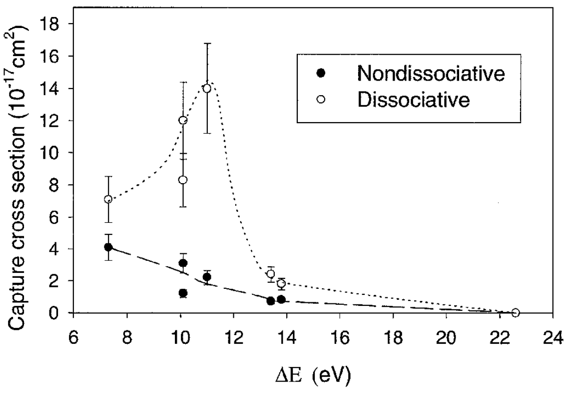

FIG. 4. Capture cross sections as functions of the electronic endoergicity ΔE. The curves are drawn to guide the eye.

internal energy. Accordingly, to a first approximation, coupling between internal rovibrational and electronic excitation energy can be neglected in the collision. The energy ΔE, which is used for electron excitation in the transfer process, is amply available as kinetic energy since the center of mass energy in the collision ranges from 72 eV in H_2 to 4.3 keV in Xe.

In summary, we have presented measurements of dissociative as well as nondissociative single electron capture by highly fluorinated fullerene anions in collisions with various target gases. The observation that anions can capture an extra electron, especially from the rare gases where the active electron is bound with more than 10 eV, is explained as a result of crossing between the potential energy curves associated with the initial and final quasimolecules.

This work was supported by the Danish National Research Foundation through the Aarhus Center of Advanced Physics (ACAP).

[1] R.K. Janev, L.P. Presnyakov, and V.P. Shevelko, in *Physics of Highly Charged Ions,* Springer Series in Electrophysics Vol. 13 (Springer-Verlag, Berlin, 1985).

[2] R.B. Moore, A.M.G. Dezfuli, P. Várfalvy, and H. Zhao, Phys. Scr. **T59**, 93 (1995).

[3] H. Shen, P. Hvelplund, D. Mathur, A. Bárány, H. Cederquist, N. Selberg, and D.C. Lorents, Phys. Rev. A **52**, 3847 (1995).

[4] C.F. Rohmund and E.E.B. Campbell, Z. Phys. D **40**, 339 (1997).

[5] R.D. Smith, J.A. Loo, R.R.O. Loo, M. Busman, and H.R. Udseth, Mass Spectrom. Rev. **10**, 359 (1991).

[6] A.A. Gakh, A.A. Tuinman, J.L. Adcock, R.A. Sachleben, and R.N. Compton, J. Am. Chem. Soc. **116**, 819 (1994).

[7] L.N. Sidorov, V.F. Bagryantsev, V.A. Seredenko, A.S. Zapol'skii, J.M. Street, and R. Taylor, J. Chem. Soc. Perkin Trans. **2**, 2275 (1996); O.V. Boltalina, A.Ya. Borschevskii, L.N. Sidorov, J.M. Street, and R. Taylor, Chem. Commun. 529 (1996); O.V. Boltalina, V.Yu. Marko, R. Taylor, and M.P. Waugh, *ibid.* 2549 (1996).

[8] O.V. Boltalina, D.B. Ponomarev, A.Ya. Borschevskii, and L.N. Sidorov, J. Phys. Chem. **101**, 2574 (1997).

[9] A.A. Tiunman, P. Mukherjee, J.L. Adcock, R.L. Hettich, and R.N. Compton, J. Phys. Chem. **96**, 7584 (1992).

[10] C. Jin, R.L. Hettich, R.N. Compton, A. Tuinman, A. Derecskei-Kovács, D.S. Marynick, and B.I. Dunlap, Phys. Rev. Lett. **73**, 2821 (1994).

[11] I.P. Malkerova, D.V. Sevast'yanov, A.S. Alikhanyan, S.P. Ionov, and N.G. Spitsyna, Dokl. Chem. **342**, 142 (1995).

[12] P. Hvelplund, L.H. Andersen, C. Brink, D.H. Yu, D.C. Lorents, and R. Ruoff, Z. Phys. D **30**, 323 (1994).

[13] R.E. Olsen and A. Salop, Phys. Rev. A **14**, 579 (1976).

[14] W.J. Griffiths, D. Mathur, and F.M. Harris, Int. J. Mass Spectrom. Ion Process. **87**, R1 (1989).

[15] O. Almén and K.O. Nielsen, Nucl. Instrum. Methods **1**, 302 (1957).

[16] O.V. Boltalina, N.A. Galeva, V.Yu. Markova, A.Ya. Borschevskiy, I.D. Sorokin, L.N. Sidorov, A. Popovich, and D. Zigon, Mendeleev Commun. (to be published).

[17] D. Bakowies and W. Thiel, Chem. Phys. Lett. **193**, 236 (1992).

[18] J.P. Fowler, J.P.B. Sandall, and R. Taylor, J. Chem. Soc. Perkin Trans. **2**, 419 (1996).

[19] R.E. Haufler *et al.*, J. Phys. Chem. **94**, 8634 (1990).

[20] H. Selig, C. Lifshitz, T. Peres, J.E. Fischer, A.R. McGhie, W.J. Romanow, J.P. McCauley, Jr., and A.B. Smith, J. Am. Chem. Soc. **113**, 5475 (1991).

[21] J.U. Andersen, C. Brink, P. Hvelplund, M.O. Larsson, B. Bech Nielsen, and H. Shen, Phys. Rev. Lett. **77**, 3991 (1996).

[22] J.H. Steger, U. Mische, W. Kamke, A. Ding, M. Fieber-Erdmann, and T. Drewello, Chem. Phys. Lett. **276**, 39 (1997).